Multi-objective optimization of composite two-stage vibration isolation system for sensitive equipment

Wei Huang
School of Civil and Hydraulic Engineering, Hefei University of Technology, Hefei, China and Anhui Provincial Laboratory of Civil Engineering and Materials, Hefei, China

Jian Xu
China National Machinery Industry Corporation, Beijing, China

Dayong Zhu and Cheng Liu
School of Civil and Hydraulic Engineering, Hefei University of Technology, Hefei, China and Anhui Provincial Laboratory of Civil Engineering and Materials, Hefei, China

Jianwei Lu
School of Mechanical and Automotive Engineering, Hefei University of Technology, Hefei, China, and

Kunlin Lu
School of Civil and Hydraulic Engineering, Hefei University of Technology, Hefei, China and Anhui Provincial Laboratory of Civil Engineering and Materials, Hefei, China

Received 2 December 2014
Revised 29 January 2015
Accepted 16 April 2015

Abstract

Purpose – The purpose of this paper is to propose a novel strategy of optimal parameters configuration and placement for sensitive equipment.

Design/methodology/approach – In this study, clamped thin plate is considered as the foundation form, and a novel composite system is proposed based on the two-stage isolation system. By means of the theory of mechanical four-pole connection, the displacement amplitude transmissibility from the thin plate to precision equipment is derived. For the purpose of performing optimal design of the composite system, a novel multi-objective idea is presented. Multi-objective particle swarm optimization (MOPSO) algorithm is adopted as an optimization technique, which can achieve a global optimal solution (*gbest*), and selecting the desired solution from an equivalent Pareto set can be avoided. Maximum and variance of the four transmitted peak displacements are considered as the fitness functions simultaneously; the purpose is aimed at reducing the amplitude of the multi-peak isolation

This research was completely supported by National Natural Science Foundation of China, and the Grant Numbers are 51078123, 51179043. Valuable comments and suggestions by preparation experts of the national code – "Code for vibration load design of industrial building" – on the ideas carried out are gratefully acknowledged.

Journal of Engineering, Design and Technology
Vol. 14 No. 2, 2016
pp. 343-361

1726-0531
DOI 10.1108/JEDT-12-2014-0074

system, meanwhile pursuing a uniform vibration as far as possible. The optimization is mainly organized as a combination of parameter configuration and placement design, and the traversal search of discrete plate is performed in each iteration for the purpose of achieving the global optimum.

Findings – An important transmissibility based on the mechanical four-pole connection is derived, and a composite vibration isolation system is proposed, and a novel optimization problem is also defined here. This study reports a novel optimization strategy combined with artificial intelligence for parameters and placement design of precision equipment, which can promote the traditional view of two-stage vibration isolation.

Originality/value – Two-stage vibration isolation systems are widely applied to the vibration attenuation of precision equipment, but in these traditional designs, vibration participation of foundation is often ignored. In this paper, participation of foundation of equipment is considered, and a coherent new strategy for equipment isolation and foundation vibration is presented. This study shows a new vision of interdisciplinary including civil engineering, mechanical dynamics and computational science.

Keywords Artificial intelligence, Mechanical engineering, Industrial engineering, Simulation modeling, Multi-objective optimization, Design implementing managing and practicing innovation, Computational mechanics, Two-stage, Vibration isolation, Sensitive equipment, Thin plate, Composite system

Paper type Research paper

1. Introduction

Growth and development of various engineering and technical industries are often geared toward improvement, which is typically achieved by focusing on improvements made to the machining process. This is closely accompanied with the development of a wide variety of application and innovation of precision and ultra-precision equipment, which is leading the new era of modern engineering. Vibration is a key problem in the process of utilizing sensitive equipment, and isolating and attenuating the harmful vibration from the surrounding environment to the equipment has played a significant role.

Passive methods are commonly utilized for vibration isolation of sensitive equipment, single-stage system of which is the most primitive method; unfortunately, the isolation system can not always enter the desired region because of the narrow frequency band. Subsequently, the two-stage isolation system is proposed, and descending speed of transmissibility is much faster than the single-stage one when the excitation frequency is greater than the second resonance frequency, which is very conducive to perform vibration isolation with this method (Shen and Yan, 1984), and the merits and ideal isolation effect are also recognized (Petrov, 1989). Meanwhile, with the fast improvement of advance in sensitive equipment, requirements for isolating the ultra-low frequency bandwidth are more stringent, and a two- or multi-stage vibration isolation system should be adopted when a single-stage one cannot meet the desired level (Nguyen, 1997). Isolation performance is closely related to the parameters configuration, and appropriate parameters can improve the isolation performance; otherwise, it will be counterproductive. Therefore, it is very necessary to perform an optimal design for the two-stage isolation system. Snowdon (1971) performed an analysis of the sinusoidal vibration of damped mechanical systems by the use of the four-pole connection, and the parameters that described the bending vibrations of a Bernoulli-Euler beam and a thin circular plate were also stated. Snowdon (1979) evaluated both the use and the characterization of the performance of anti-vibration mountings for the control of noise and vibration, and a discussion was then given about

the two-stage system. Wei *et al.* (2006) performed parameters optimization for the two-stage vibration isolation system with a combined method of maximum entropy and genetic algorithm, and a hybrid numerical method for the two-stage vibration isolation design was proposed. Utilization of maximum entropy method for processing non-differentiable optimization was also studied for the two-stage vibration isolation, and the numerical cases could give inspiration (Chen *et al.*, 2001). Song *et al.* (2010) presented an implementation of an air-bearing, two-stage system and its control strategy, and the identification and control design were introduced in detail. In addition, the results showed that the proposed strategy could achieve a high-speed, ultra-precision linear motion with a satisfactory performance. Bronowicki *et al.* (2003) proposed a two-stage passive isolation approach using isolation first at the vibration-inducing reaction wheels, and a second isolation layer between the bus portion of the space vehicle (the backpack) and the optical payload for the space-based optical instruments. Parameters optimization for a two-stage mounting isolation system was studied, and in which the maximum entropy approach was also applied (Chen *et al.*, 2001). Moore (2011) derived the equations of motion for generalized two-stage and two-stage rafted vibration isolation systems using a matrix methodology, and the supported mass and intermediate masses were assumed to be rigid and supported by isolators with arbitrary locations and orientations.

Seen from the aforementioned presentations, traditional isolation design is generally based on the assumption that the foundation is not involved in the vibration of affiliated equipment; in other words, it is always considered absolutely rigid. However, the vibration isolation will not reach an ideal level when an external high-frequency stimulus and low stiffness of foundation exist. Therefore, vibration participation of foundation must be taken into account in engineering practice. Thin plate is a common foundation form of equipment, which is simply supported for the sake of calculation simplicity in general; however, the clamped form cannot be ignored for its wide range of applications, such as the floors of industrial buildings. Amabili *et al.* (2012) performed a study of large-amplitude forced vibration of a clamped stainless steel plate excited by centralized harmonic force. Civalek *et al.* (2009) performed free vibration analysis of annular Mindlin plates with free inner edge, and the discrete singular convolution method was used for discretization of equations of motion. A comparative study of active and passive vibration isolation of clamped thin plate was conducted, which was aimed at examining piezoelectric materials in active vibration control (Kozupa and Wiciak). A free vibration problem of clamped thin plate was solved by using quasi Green function (Li and Yuan, 2012). Arenas (2003) derived a general numerical expression of clamped thin plate vibration with virtual work principle, in which simultaneous equations were avoided, and the solutions were easy to be calculated and programmed; meanwhile, complex symmetric characteristic of the Rayleigh–Ritz method could be overcome.

In general, the traditional gradient-based optimization requires the computations of sensitivity factors and eigenvectors at its iteration process. This causes heavy computational burden and slow convergence. Moreover, there is no local criterion to decide whether a local solution is also the global solution. Thus, the conventional optimization methods using derivatives and gradients are generally not able to locate or identify the global optimum; however, for real-world applications, one is often content with a good solution, even if it is not the best solution. Consequently, heuristic methods are widely used for the global optimization problem. Particle swarm optimization (PSO) algorithm was first

proposed by Eberhart and Kennedy (1995), and it is a novel population-based metaheuristic, utilizing the swarm intelligence generated by the cooperation and competition between the particles in a swarm, and has emerged as a useful tool for engineering optimization. Sun *et al.* (2014a) proposed an adaptive particle swarm optimization method (APSO), and this technique was applied to improve the global optimization performance based on the hypothesis testing. As an application of PSO, active vibration isolation reducing vibration transmitted from vibrating base to sensitive equipment was investigated, and the fitness using H_∞ control criterion was presented as a cost function and then optimized by the PSO algorithm (Farshidianfar *et al.*, 2012). This study can be a representative of the rise of PSO technique in equipment isolations, but such researches are still few.

Coello *et al.* (2002) first proposed the multi-objective particle swarm optimization (MOPSO) algorithm, and the main idea is that by determining the flying direction of the particles with optimal Pareto sets and non-dominated solutions in the global knowledge base found before, the particle flying can be guided, and a unique, optimal and global solution can be obtained by use of a specific algorithm. MOPSO can overcome some disadvantages of traditional multi-objective methods (such as strength Pareto evolutionary algorithm (SPEA) and SPEA2), and a desired solution selected from a group of equivalent Pareto set is solved (Fonseca and Fleming, 1995). Applications of MOPSO have been extensively performed in many areas, for example structural vibration control (Marinaki *et al.*, 2011), power transmission and transformation (Sun *et al.*, 2014a), active suspension of vehicle system (Rajagopal and Ponnusamy, 2014), etc. However, the application of MOPSO in vibration suppression of equipment is rare, and the researches involved in this can be considered as a prospect.

In this paper, vibration participation of foundation is considered, and a novel composite two-stage vibration isolation system is proposed, and a key factor – transmissibility – is derived based on the mechanical four-pole connection. For the purpose of performing optimal design of the proposed system, a multi-objective optimization problem is defined, and the MOPSO technique is adopted here; furthermore, detailed numerical verifications are also presented.

2. Brief introductions to MOPSO

PSO was originated from the predatory behavior of birds, and each solution of the optimization problem was regarded as a bird in the search space, which could be referred to as *particle*. Each particle has its own speed and position vector (determine the direction and distance of flight), and a current optimum *pbest* can be found according to fitness computation. With the ongoing flight, the best position of the entire swarm can be updated, and a global and optimal value *gbest* is obtained (*gbest* is the optimum of *pbest*).

In the PSO algorithm, own state of every particle can be described by a group of position and velocity vectors which, respectively, represent the possible solutions and motion directions in the searching space. By constantly learning the found global and optimal solutions and the moving directions, also updating the neighbor optimal solutions, the desired solution can be obtained. The main steps of MOPSO can be summarized as follows:

- *Step 1*: Initialize the population, compute the corresponding objective vectors of particles and add the non-dominated solutions to the external archive.
- *Step 2*: Initialize the local optimum *pbest* of particles and the global optimum *gbest*.

- *Step 3*: Amend the velocities and positions of the particles by evaluating the following equations so as to generate new *pbest*:

$$v_{ij} = \omega v_{ij}(t) + c_1 r_1 (pbest_{ij}(t) - x_{ij}(t)) + c_2 r_2 (gbest_{ij}(t) - x_{ij}(t)) \quad (1)$$

$$x_{ij}(t+1) = x_{ij}(t) + v_{ij}(t+1) \quad (2)$$

where i represents the ith particle; j represents the jth dimension of each particle; t represents the tth generation; $v_{ij}(t)$ represents the flight velocity vector; $x_{ij}(t)$ represents the flight displacement vector; *pbest* represents the optimal location component; *gbest* represents the optimal position of the entire particle swarm; c_1,c_2 are acceleration factors or learning factors; and r_1,r_2 are random numbers between (0,1). ω is the inertia weight factor, which plays a key role in the PSO.

- *Step 4*: Maintain the external archive with the obtained new non-dominated solution, and select *gbest* for every particle (the archive determines the selection of the global optimum).
- *Step 5*: Whether the maximum iteration is reached; if no, the program will continue; if yes, terminate the computation, and output the optimal Pareto solution set and the *gbest*.

It is important to point out that MOPSO is essentially different with PSO, and the main difference is focused on the selecting of global optimum and the setting and updating of external archives; it is worth mentioning that the archives determine the global optimum. The rule of archive updating is briefly shown in Figure 1.

Parsopoulos and Vrahatis (2002) proposed a MOPSO algorithm based upon target aggregation, which transferred the multi-objective optimization problem to a single-objective problem using a fixed and adaptive weight. Fieldsend and Singh (2002) presented a data structure of dominated tree, by use of which, an elite solution was saved and the optimal experience of particles was selected. Li (2003) introduced the main idea of NSGA-2 into PSO for the purpose of accomplishing the multi-objective optimization, but the result was merely closed to NSGA-2. Pareto dominance is a most direct way to obtain a desired optimum from a group of continuous solutions, namely, consider all of the non-dominated solutions in the archive, and determine a "leader", and then a Pareto frontier generates, which can be schematically seen in Figure 2. Density measuring technique is commonly used to determine the global optimum, and the nearest neighbor density estimation method (Deb *et al.*, 2002) based on the nearest neighbor congestion

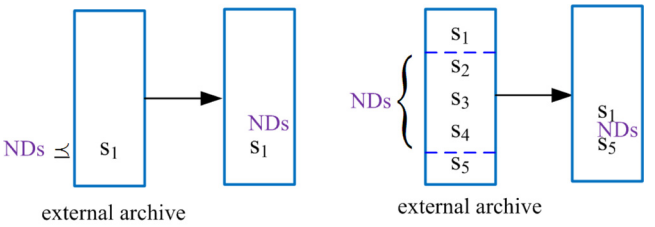

Note: NDs denotes non-dominated set and s_1~s_5 denotes a group of solutions

Figure 1.
The rule of archive updating

evaluation of particles is adopted in this paper. Certainly, there are also other similar methods, such as kernel density estimation method (Goldberg and Richardson, 1987).

3. Composite two-stage vibration isolation system

Schematic of two-stage vibration isolation system for typical sensitive equipment is shown in Figure 3.

Figure 3(a) shows typical sensitive equipment used in high-resolution microscopy. Such equipment is widely applied in various areas, including biological and chemical engineering. This kind of equipment is vibration-sensitive and any small external disturbance can affect the accuracy and quality.

In Figure 3(b), ① denotes the sensitive equipment, ② denotes the first-stage isolators, ③ denotes the intermediate block or platform, ④ denotes the second-stage isolators and ⑤ denotes the clamped thin plate foundation. m_1 is the mass of equipment which is supported by four isolators mounted on the intermediate mass; the stiffness and damping of ② can be denoted as k_1 and c_1; m_2 is the intermediate mass; and the stiffness and damping of ④ can be denoted as k_2 and c_2. The geometry of the thin plate is $a \times b \times h$, and the equipment can be simplified as a cuboid (plane size is $e \times f$, and the size of intermediate block is assumed the same). The centralized harmonic excitation force on the plate is $Fe^{j\omega t}$, F is the amplitude and ω is the circular frequency. ①~⑤ are considered as a composite isolation system which can be expressed in Cartesian coordinates (shown in Figure 4), O is the coordinate origin and A, B, C and D are, respectively, the four corner installations of sensitive equipment.

Seen from Figure 5, according to the four-pole connection (Snowdon, 1971; Yan, 1985), Systems 1 and 2 can be deemed series, and for each individual system, the four-pole expression can be written, respectively, as:

$$S_1 = [k_{1ij}{}^*][m_{1ij}]; S_2 = [k_{2ij}{}^*][m_{2ij}] \tag{3}$$

where $[m_{1ij}]$ and $[m_{2ij}]$ are the four-pole parameters of mass and $[k_{1ij}{}^*]$ and $[k_{2ij}{}^*]$ are the four-pole parameters of the stiffness and damping in parallel; thus, the four-pole connection of the two systems in series can be derived as:

$$\begin{bmatrix} F_1 \\ X_1 \end{bmatrix} = S_1 S_2 \begin{bmatrix} F_{end} \\ X_{end} \end{bmatrix} \tag{4}$$

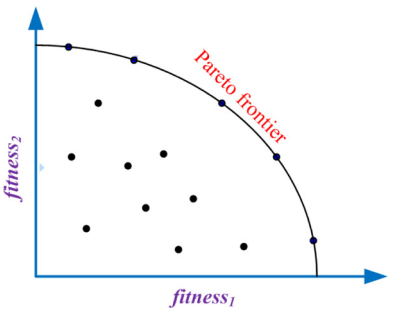

Figure 2.
Non-dominated set with Pareto frontier

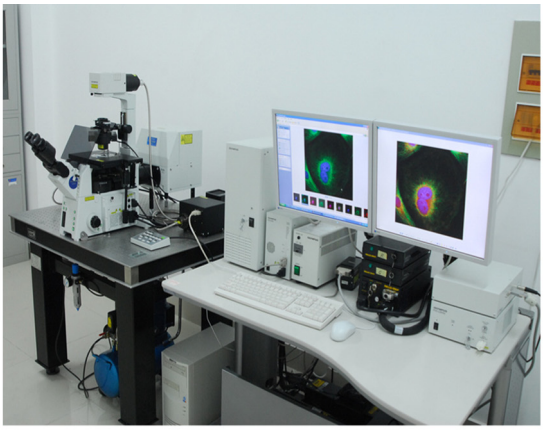

(a)

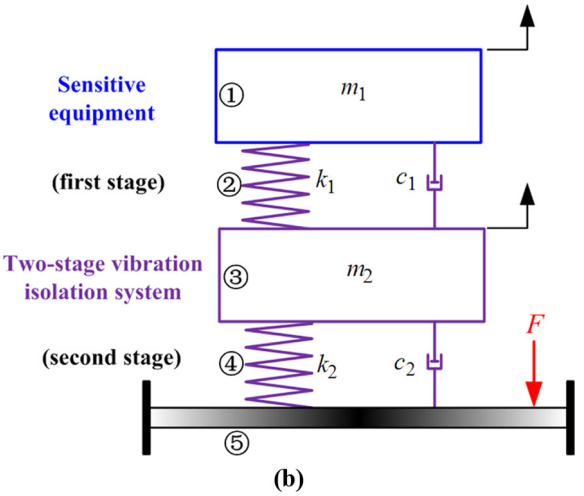

(b)

Notes: (a) Physical map of a typical sensitive equipment; (b) simplified model

Figure 3.
Composite two-stage vibration isolation system

Where:

$$[k_{1ij}^*] = \begin{bmatrix} 1 & 0 \\ \dfrac{1}{k_1 + ic_1\omega} & 1 \end{bmatrix}, [m_{1ij}] = \begin{bmatrix} 1 & -m_1\omega^2 \\ 0 & 1 \end{bmatrix};$$

$$[k_{2ij}^*] = \begin{bmatrix} 1 & 0 \\ \dfrac{1}{k_2 + ic_2\omega} & 1 \end{bmatrix}, [m_{2ij}] = \begin{bmatrix} 1 & -m_2\omega^2 \\ 0 & 1 \end{bmatrix}.$$

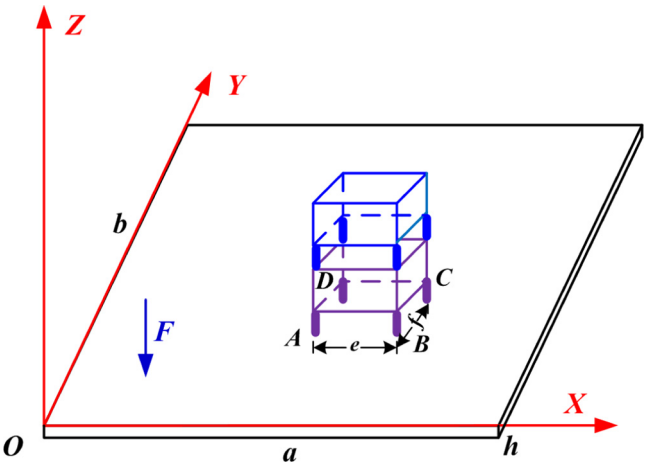

Figure 4.
Schematic of the proposed composite vibration isolation system expressed in Cartesian coordinate system

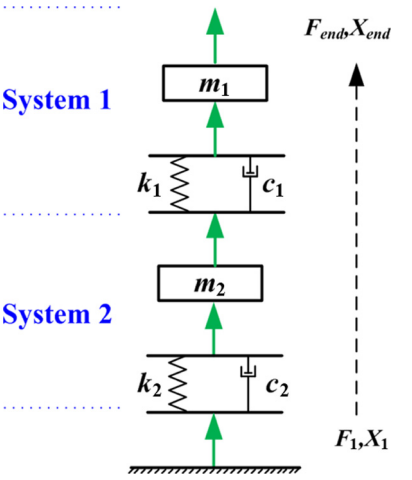

Figure 5.
Schematic of four-pole connection

The following can be derived by transforming equation (4) as follows:

$$X_1 = \Omega_{21} F_{end} + \Omega_{22} X_{end} \tag{5}$$

Suppose $F_{end}/X_{end} = Z_m$ (Z_m denotes the mechanical impedance of sensitive equipment), and $u = m_1/m_2$, $n_1 = k_1/k_2$, $n_2 = c_1/c_2$, $\omega_{n2} = \sqrt{k_2/m_2}$, $\xi_2 = c_2/(2m_2\omega_{n2})$ and $\theta = \omega_{n2}/\omega$; then, by dividing both the sides of equation (5) with X_{end}, the displacement transmissibility can be derived as:

$$T_d = \left| \frac{X_{end}}{X_1} \right| = 1 \Big/ \sqrt{\frac{C_1^2 + C_2^2}{C_3^2 + C_4^2}} \tag{6}$$

where:

$$C_1 = A_1B_3Z_m - A_2B_4Z_m + A_3B_1 - A_4B_2;$$
$$C_2 = A_1B_4Z_m + A_2B_3Z_m + A_4B_1 + A_3B_2;$$
$$C_3 = A_3B_3Z_m - A_4B_4;$$
$$C_4 = A_3B_4 + A_4B_3.$$

where:

$$A_1 = n_1 + 1 - u\theta^2;$$
$$A_2 = n_2 \times 2\xi_2\theta + 2\xi_2\theta;$$
$$A_3 = n_1k_2 - n_2 \times 2\xi_2c_2\theta\omega;$$
$$A_4 = n_1k_2 \times 2\xi_2\theta + k_2n_2 \times 2\xi_2\theta;$$
$$B_1 = -\theta^2 + n_1 - n_1\theta^2 - u\theta^2 + u\theta^4 - n_2(2\xi_2)^2\theta^2;$$
$$B_2 = -2\xi_2\theta^3 + n_1 \times 2\xi_2\theta + n_2 \times 2\xi_2\theta - n_2 \times 2\xi_2\theta^3 - u \times 2\xi_2\theta^3;$$
$$B_3 = n_1 - n_2(2\xi_2)^2\theta^2;$$
$$B_4 = n_1 \times 2\xi_2\theta + n_2 \times 2\xi_2\theta.$$

(Detailed derivation is presented in Appendix.)

Seen from equation (6), T_d is a complex function with multiple variables $u, n_1, n_2, \xi_2, k_2, c_2, \theta, \omega, m_1, Z_m$. In a specific working condition, ω, m_1, Z_m can be regarded as constants; in addition, θ is an intermediate variable which can be derived by other parameters; in the meantime, $c_2(= 2\xi_2\omega_{n2}m_2)$ can be also regarded as a constant; thus, T_d can be simply referred to as $\Gamma(u, n_1, n_2, \xi_2, k_2)$.

4. Proposed solution of clamped thin plate vibration

Based on the virtual work principle, Arenas derived a general form of displacement solutions of clamped thin plate excited by centralized harmonic force:

$$X(x,y) = F\sum_{m=1}^{\infty}\sum_{n=1}^{\infty}\frac{\Psi_{mn}(x,y)\Psi(x',y')}{B(I_1I_2 + 2I_3I_4 + I_5I_6) - \rho_s\omega^2I_2I_6} \tag{7}$$

where $B = Eh^3/[12(1 - \upsilon^2)]$ is the bending stiffness of thin plate; E is the Young's modulus; υ is the Poisson's ratio; $\rho_s = \rho h$ is the surface density of thin plate, and ρ is the volume density; (x,y) is a random discrete point on the plate; and (x',y') is the position of external disturbance.

In practice, the infinite series in equation (7) are often truncated into a finite term, and in this paper, $m, n = 1, 2, \ldots, 6$.

Modal function $\Psi_{mn}(x,y)$ is denoted as:

$$\Psi_{mn}(x,y) = \theta_m(x)\xi_n(y) \tag{8}$$

where $\theta_m(x) = J(\beta_m x/a) - J(\beta_m)/H(\beta_m)H(\beta_m x/a), \zeta_n(y) = J(\beta_n y/b) - J(\beta_n)/H(\beta_n)H(\beta_n y/b)$.

$J(\bullet) = \cosh(\bullet) - \cos(\bullet), H(\bullet) = \sinh(\bullet) - \sin(\bullet)$; and β_i is the root of the formula $\cosh(\beta)\cos(\beta) = 1$.

$$I_2 I_6 = \frac{ab}{\beta_m \beta_n} L_m L_n; I_3 I_4 = \frac{\beta_m \beta_n}{ab} R_m R_n; I_1 = I_6 \left(\frac{\beta_m}{a}\right)^4; I_5 = I_2 \left(\frac{\beta_n}{b}\right)^4;$$

$$L_i = \frac{(1 + D_i^2)\sinh(2\beta_i)}{4} + \sinh(\beta_i)[2D_i \sin(\beta_i) - (1 - D_i^2)\cos(\beta_i)] - (1 + D_i^2)\sin(\beta_i)\cosh(\beta_i) + (1 - D_i^2)\sin(\beta_i)\cos(\beta_i) + \beta_i - \frac{D_i[1 + \cosh(2\beta i)]}{2} + Di\cos^2(\beta_i);$$

$$R_i = \frac{(1 + D_i)^2 \sinh(2\beta_i)}{4} - \frac{D_i \cosh(2\beta_i)}{2} - \frac{(1 - D_i^2)\sin(\beta_i)\cos(\beta_i)}{2} - D_i \cos^2(\beta_i) - D_i^2 \beta_i + \frac{3D_i}{2}; D_i = \frac{J(\beta_i)}{H(\beta_i)}.$$

5. Parameters and placement optimization using MOPSO technique

In traditional studies, the isolated objects are often simplified as a mass dot; however, size of the equipment in practice cannot be ignored with respect to the foundation. As shown in Figure 4, transmitted vibration from thin plate to intermediate mass (then to sensitive equipment) will bring about four different amplitudes which are extremely unfavorable for the normal use and maintenance of sensitive equipment. Therefore, transmitted vibration to sensitive equipment must be reduced as far as possible; meanwhile, the different vibrations should be more uniform. Finally, a multi-objective problem can be summarized.

In Figure 4, the original displacements of A, B, C and D of thin plate can be denoted as X_A, X_B, X_C and X_D, respectively, and the transmitted displacements to sensitive equipment can be, respectively, denoted as $X_{m2A} = |T_{dA}|X_A$, $X_{m2B} = |T_{dB}|X_B$, $X_{m2C} = |T_{dC}|X_C$ and $X_{m2D} = |T_{dD}|X_D$, and the transmissibility can be derived by use of the principle described in Section 3.

The two fitness functions can be written as:

$$\begin{cases} fitness_1 = \max(|X_{m2A}, X_{m2B}, X_{m2C}, X_{m2D}|) \\ fitness_2 = \text{var}(X_{m2A}, X_{m2B}, X_{m2C}, X_{m2D}) \end{cases} \tag{9}$$

where max (•) and var (•) are operations based on MATLAB2010.

Note: max (X) generates the maximum value of **X** (**X** is a vector). var (X) computes the variance of **X** (**X** is a sample).

Figure 6 shows the discrete grid of thin plate and the schematic placement of sensitive equipment.

The basic strategy of multi-objective optimization is organized in Figure 7.

5.1 Numerical example

The basic parameters of thin plate are set as $a = 3.0m, b = 6.0m, h = 0.2m$, $\rho = 7{,}800kg/m^3$, $\upsilon = 0.33$, $E = 2.1\times10^{11}Pa$. The force amplitude is $F = 10N$; the circular frequency is $\omega = 2\pi$ rad/s; and the coordinate of external disturbance is z (0.5454m, 0.9765m). Discretize the thin plate so as to obtain the coordinates (x,y) of all points on the plate, and the accuracies are, respectively, denoted as Δx, Δy:

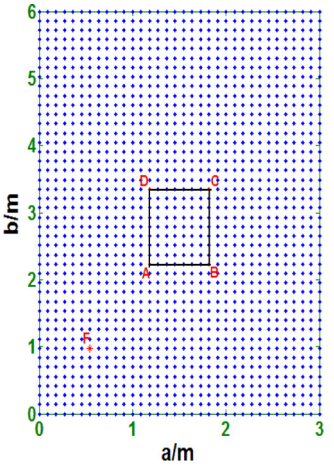

Figure 6.
Discrete grid of thin plate

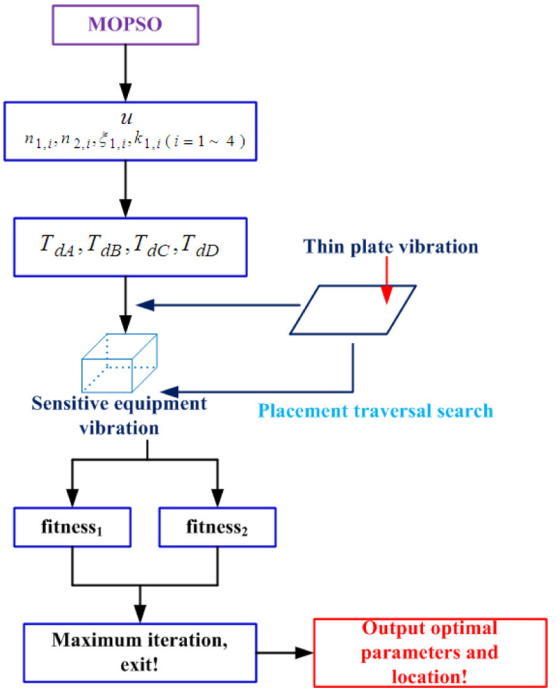

Figure 7.
Idea chart of the multi-objective optimization

$$\Delta x = linspace\,(0, a, 34),$$
$$\Delta y = linspace\,(0, b, round\ (b/a \times 22);$$

(*linspace* (·), *round* (·) are respectively the operations based on MATLAB2010)

Note: *linspace* (x_1,x_2,N) equally generates N spaced points between x_1 and x_2; *round*(x) rounds the element of x to the nearest integer.

The forced vibration of thin plate with discrete grid is schematically shown in Figure 8, which will cause vibration of sensitive equipment, and the proposed multi-objective optimization will be performed subsequently based on this.

The mass of sensitive equipment is supposed as $m = 50kg$; the mechanical impedance is $Z_m = 2000\Omega$; and the plane size is $e \times f = 0.71 \times 1.10m$ (assume that the size of intermediate mass is equal to the sensitive equipment in this study). For the two-stage isolators installed at A, B, C and D, the undetermined parameters to be optimized can be denoted as:

$$\text{Mass ratio: } u;$$
$$\text{Two-stage isolators: } n_{1,i}, n_{2,i}, \xi_{1,i}, k_{1,i} (i = 1 \sim 4).$$

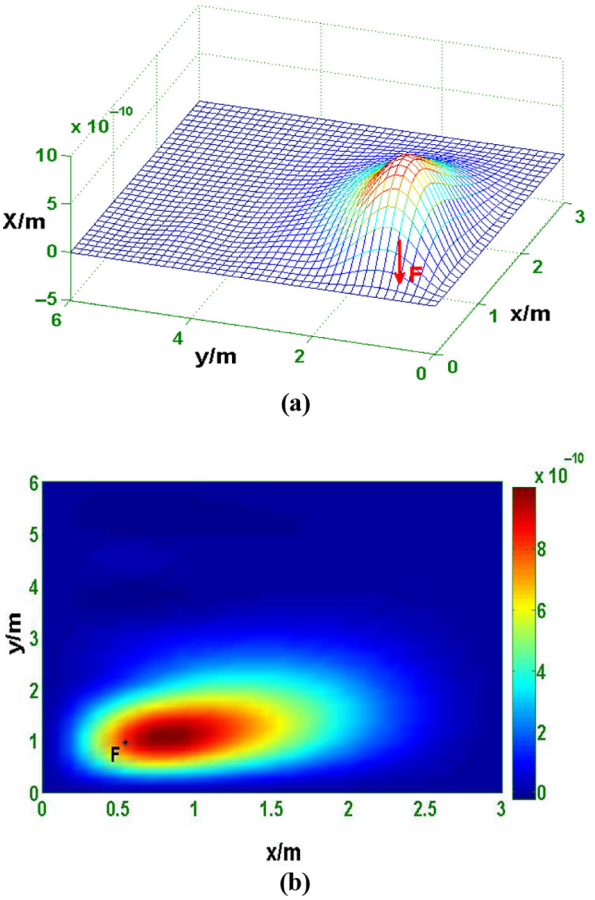

Figure 8.
Schematic of thin plate vibration

Notes: (a) Plate vibration with discrete grid; (b) plate vibration with pseudo-color contour

The dimension of MOPSO algorithm is 17, which is corresponding to:

$$swarm(1) = u;$$
$$swarm(t+1) = n_{1,t}; swarm(t+2) = n_{2,t}; swarm(t+3) = \xi_{2,t};$$
$$swarm(t+4) = k_{2,t}(t = 1, 5, 9, 13).$$

The searching scope is arbitrarily set as:

[1e-2,1e-2,1e-2,1e-2,1,1e-2,1e-2,1e-2,1,1e-2,1e-2,1e-2,1,1e-2,1e-2,1e-2,1]~
[1e2,1e2,1e2,1e2,1e6,1e2,1e2,1e2,1e6,1e2,1e2,1e2,1e6,1e2,1e2,1e2,1e6].

The population size is 200; the maximum iteration is 100; and the learning factors are defined as $c_1 = 1.5$, $c_2 = 1.5$. Linear changing strategy is utilized for inertia weight factor (Shi and Eberhart, 1998), and $\omega_{max} = 0.9$, $\omega_{min} = 0.4$.

In this paper, the presented equipment is non-equilateral, which is aimed at simulating a general case, and the following two placement conditions are involved.

Case 1, the short size e of equipment is in parallel with the short size a of thin plate; and

Case 2, the short size e of equipment is in parallel with the long size b of thin plate.

The optimization results of the presented two cases are listed in Figures 9 and 10.

The *gbest* solution of Case 1 is:

[64.4275,
52.2822, 38.7865, 29.7434, 9.8448×10^4,
21.5166, 22.7125, 9.0775, 1.8513×10^5,
11.9378, 47.0243, 31.5165, 3.4975×10^4,
22.6317, 48.4077, 20.8889, 1.0169×10^5].

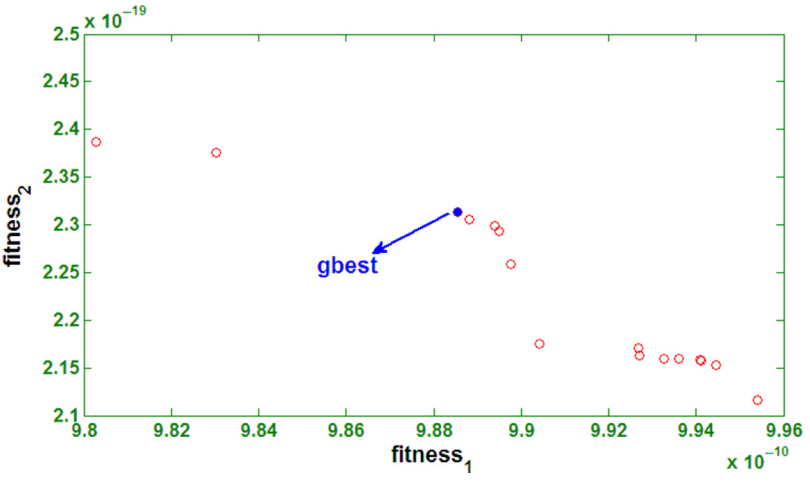

Figure 9.
Pareto frontier with *gbest* solution (Case 1)

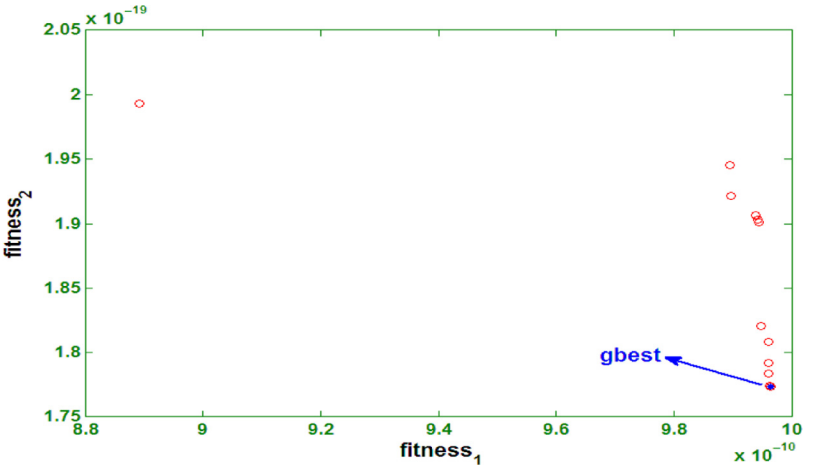

Figure 10.
Pareto frontier with *gbest* solution (Case 2)

Then, the stiffness of first-stage isolators can be derived as:

$$k_{A1} = 5.1471 \times 10^6 N/m, k_{B1} = 3.9835 \times 10^6 N/m,$$
$$k_{C1} = 4.1752 \times 10^5 N/m, k_{D1} = 2.3015 \times 10^6 N/m,$$

and the damping parameters are:

$$c_{A1} = 6.3775 \times 10^5 \mathrm{N}{\cdot}s/m, c_{B1} = 1.5630 \times 10^5 \mathrm{N}{\cdot}s/m,$$
$$c_{C1} = 4.8834 \times 10^5 \mathrm{N}{\cdot}s/m, c_{D1} = 5.6814 \times 10^5 \mathrm{N}{\cdot}s/m.$$

The stiffness of second-stage isolators can be derived as:

$$k_{A2} = 9.8448 \times 10^4 N/m, k_{B2} = 1.8513 \times 10^5 N/m,$$
$$k_{C2} = 3.4975 \times 10^4 N/m, k_{D2} = 1.0169 \times 10^5 N/m,$$

and the damping parameters are:

$$c_{A2} = 1.6442 \times 10^4 \mathrm{N}{\cdot}s/m, c_{B2} = 6.8817 \times 10^3 \mathrm{N}{\cdot}s/m,$$
$$c_{C2} = 1.0384 \times 10^4 \mathrm{N}{\cdot}s/m, c_{D2} = 1.1736 \times 10^4 \mathrm{N}{\cdot}s/m.$$

After isolation, the peak displacements of A, B, C and D transmitted to sensitive equipment are, respectively:

$$X_{A,\max} = 9.8792 \times 10^{-10} m, X_{B,\max} = 5.7295 \times 10^{-10} m,$$
$$X_{C,\max} = 3.3022 \times 10^{-10} m, X_{D,\max} = 2.4731 \times 10^{-10} m;$$

and the variance of peak displacements is 1.1042×10^{-19}. Optimal placement of equipment is obtained simultaneously by traversal searching, and the coordinates are $A(0.8181m, 1.1160m)$, $B(1.5281m, 1.1160m)$, $C(1.5281m, 2.2160m)$ and $D(0.8181m, 2.2160m)$.

The *gbest* solution of Case 2 is:

$$\begin{bmatrix} 45.8249, \\ 31.8236, 4.1021, 46.0567, 3.3256 \times 10^5, \\ 29.0805, 62.9704, 3.9573, 1.0901 \times 10^4, \\ 31.5520, 1.5888, 13.6522, 2.7444 \times 10^4, \\ 71.1200, 89.5540, 2.2642, 5.6669 \times 10^5 \end{bmatrix}.$$

The stiffness of first-stage isolators can be derived as:

$$k_{A1} = 1.0583 \times 10^7 N/m, k_{B1} = 3.1699 \times 10^5 N/m,$$
$$k_{C1} = 8.6592 \times 10^5 N/m, k_{D1} = 4.0303 \times 10^7 N/m,$$

and the damping factors are, respectively:

$$c_{A1} = 2.2762 \times 10^5 \text{N}\cdot s/m, c_{B1} = 5.4353 \times 10^4 \text{N}\cdot s/m,$$
$$c_{C1} = 7.5073 \times 10^3 \text{N}\cdot s/m, c_{D1} = 3.1889 \times 10^5 \text{N}\cdot s/m.$$

The stiffness of second-stage isolators can be derived as:

$$k_{A2} = 3.3256 \times 10^5 N/m, k_{B2} = 1.0901 \times 10^4 N/m,$$
$$k_{C2} = 2.7444 \times 10^4 N/m, k_{D2} = 5.6669 \times 10^5 N/m,$$

and the damping factors are, respectively:

$$c_{A2} = 5.5487 \times 10^4 \text{N}\cdot s/m, c_{B2} = 8.6316 \times 10^2 \text{N}\cdot s/m,$$
$$c_{C2} = 4.7249 \times 10^3 \text{N}\cdot s/m, c_{D2} = 3.5609 \times 10^3 \text{N}\cdot s/m.$$

After isolation, the peak displacements of A, B, C and D transmitted to sensitive equipment are, respectively:

$$X_{A,\max} = 9.9459 \times 10^{-10} m, X_{B,\max} = 2.9830 \times 10^{-10} m,$$
$$X_{C,\max} = 3.2833 \times 10^{-10} m, X_{D,\max} = 5.2073 \times 10^{-10} m;$$

and the variance of this sample is 1.0338×10^{-19}. Similarly, the optimal placement of equipment can be obtained as:

$A(0.8181m, 1.1160m)$, $B(1.9181m, 1.1160m)$, $C(1.9181m, 1.8260m)$, $D(0.8181m, 1.8260m)$.

Seen from the results, maximum of peak displacements of Case 1 is a little lower than Case 2, but the variance of former one is higher; all in all, this consideration is often ignored, but it should be taken into account in practice.

5.2 Further discussions

In theory, more fine mesh of thin plate can lead to more reasonable placement of sensitive equipment; however, a moderate accuracy of discrete grid is adopted here from the standpoint of computation efficiency. In addition, arbitrary installation style can be considered if the plate is of unlimited fine mesh, namely, the equipment is not requested to be in parallel with thin plate; but it is quite uneasy to perform this method with general mesh accuracy, because making the searched placement match the size of equipment well is quite difficult and the generated error may be large, and it is just ideal for numerical computation.

It is also worth mentioning that the isolated equipment is considered as four-point supporting here, but the optimization idea will be completely same for other methods (such as six-point and eight-point).

6. Conclusions

In this paper, theoretical research of clamped plate vibration is combined with isolation system of sensitive equipment, and a novel composite system based on two-stage vibration isolation is proposed, which is aimed at simulating the micro vibration disturbed by surrounding environment. A novel multi-objective optimization tool – MOPSO – is adopted here, and a unique *gbest* solution is obtained. Lower amplitude and more uniform vibration of the multi-peak system are defined as the objectives, and this strategy is validated numerically. Complex expression of transmissibility is derived based on the theory of mechanical four-pole connection, which plays a key role in the proposed system.

This study provides a broader idea for traditional isolation, and it also has certain significance in practical design of industrial manufacturing. Especially, the artificial intelligence combined with traditional isolation technique can give a lot of inspiration.

References

Amabili, M. and Carra, S. (2012), "Experiments and simulations for large amplitude vibrations of rectangular plates carrying concentrated masses", *Journal of Sound and Vibration*, Vol. 331 No. 1, pp. 155-166.

Arenas, J.P. (2003), "On the vibration analysis of rectangular clamped plates using the virtual work principle", *Journal of Sound and Vibration*, Vol. 266 No. 4, pp. 912-918.

Bronowicki, A.J., MacDonald, R., Gursel, Y., Goullioud, R., Neville, T. and Platus, P.L. (2003), "Dual stage passive vibration isolation for optical interferometer missions", *Proceedings of Astronomical Telescopes and Instrumentation, International Society for Optics and Photonics, Waikoloa, HI*, pp. 753-763.

Chen, X., Qi, H. and Zhang, Y. and Wu, C. (2001), "Optimal design of a two-stage mounting isolation system by the maximum entropy approach", *Journal of Sound and Vibration*, Vol. 243 No. 4, pp. 591-599.

Chen, X.J., Qi, H., Wu, C.J. and Qi, A.H. (1999), "Optimal design of two-stage mounting isolation system with maximum entropy approach", *Vibration and Shock*, Vol. 18 No. 4, pp. 46-50.

Civalek, Ö. and Gürses, M. (2009), "Free vibration of annular Mindlin plates with free inner edge via discrete singular convolution method", *Arabian Journal for Science and Engineering*, Vol. 34 No. 1, pp. 81-90.

Coello, C.A. and Lechuga, M.S. (2002), "MOPSO: a proposal for multiple objective particle swarm optimization", *Proceedings of the 2002 Congress on IEEE, Honolulu, HI*, pp. 1051-1056.

Deb, K., Pratap, A., Agarwal, S. and Meyarivan, T. (2002), "A fast and elitist multi-objective genetic algorithm: NSGA-II", *IEEE Transactions on Evolutionary Computation*, Vol. 6 No. 2, pp. 182-197.

Eberhart, R.C. and Kennedy, J. (1995), "A new optimizer using particle swarm theory", *Proceedings of the Sixth International Symposium on Micro Machine and Human Science*, *Nagoya*, pp. 39-42.

Farshidianfar, A., Saghafi, A., Kalami, S.M. and Saghafi, I. (2012), "Active vibration isolation of machinery and sensitive equipment using control criterion and particle swarm optimization method", *Meccanica*, Vol. 47 No. 2, pp. 437-453.

Fieldsend, J.E. and Singh, S. (2002), "A multi-objective algorithm based upon particle swarm optimization, an efficient data structure and turbulence", UK Workshop on Computational Intelligence (UKCI'02), Birmingham, pp. 37-44.

Fonseca, C.M. and Fleming, P.J. (1995), "An overview of evolutionary algorithms in multi-objective optimization", *Evolutionary Computation*, Vol. 3 No. 1, pp. 1-16.

Goldberg, D.E. and Richardson, J. (1987), "Genetic algorithms with sharing for multimodal function optimization", *Proceedings of the Second International Conference on Genetic Algorithms and Their Applications*, *MA*, pp. 41-49.

Kozupa, M.M. and Wiciak, J.W. (2011), "Comparison of passive and active methods for minimization of sound radiation by vibrating clamped plate", *Acta Physica Polonica, A*, Vol. 119, pp. 1013-1017.

Li, S. and Yuan, H. (2012), "Green quasifunction method for free vibration of clamped thin plates", *Acta Mechanica Solida Sinica*, Vol. 25 No. 1, pp. 37-45.

Li, X. (2003), "A non-dominated sorting particle swarm optimizer for multi-objective optimization", Genetic and Evolutionary Computation – GECCO 2003, Heidelberg, Berlin, pp. 37-48.

Marinaki, M., Marinakis, Y. and Stavroulakis, G.E. (2011), "Fuzzy control optimized by a multi-objective particle swarm optimization algorithm for vibration suppression of smart structures", *Structural and Multidisciplinary Optimization*, Vol. 43 No. 1, pp. 29-42.

Moore, S. (2011), "Analytical modeling of single and two-stage vibration isolation systems", *Proceedings of Acoustics, Gold Coast*, pp. 1-8.

Nguyen, T.T. (1997), "Parametric harmonic analysis of power systems", *IEEE Proceedings of Generation, Transmission and Distribution*, Vol. 144 No. 1, pp. 21-25.

Parsopoulos, K.E. and Vrahatis, M.N. (2002), "Particle swarm optimization method in multi-objective problems", *Proceedings of the 2002 ACM Symposium on Applied Computing*, *New York, NY*, pp. 603-607.

Petrov, L.F. (1989), "Analysis of nonlinear two degree-of-freedom vibration isolation system", *Vibration Engineering*, Vol. 3 No. 1, pp. 115-118.

Rajagopal, K. and Ponnusamy, L. (2014), "Multi objective optimization of vehicle active suspension system using DEBBO based PID controller", *International Journal of Engineering & Technology*, Vol. 6 No. 1, pp. 252-261.

Shen, R.Y. and Yan, J.K. (1984), "Response of two-stage vibration isolation system to base excitation of white noise", *Vibration and Shock*, Vol. 2, pp. 59-68.

Shi, Y. and Eberhart, R. (1998), "A modified particle swarm optimizer", IEEE World Congress on Computational Intelligence, Anchorage, AK, pp. 69-73.

Snowdon, J.C. (1971), "Mechanical four-pole parameters and their application", *Journal of Sound and Vibration*, Vol. 15 No. 3, pp. 307-323.

Snowdon, J.C. (1979), "Vibration isolation: use and characterization", *The Journal of the Acoustical Society of America*, Vol. 66 No. 5, pp. 1245-1274.

Song, Y., Wang, J., Yang, K., Yin, W. and Zhu, Y. (2010), "A dual-stage control system for high-speed, ultra-precise linear motion", *The International Journal of Advanced Manufacturing Technology*, Vol. 48 Nos 5/8, pp. 633-643.

Sun, K., Xu, K., Zheng, Z.M., Ding, X.Y., Sun, K., Chen, H.W. and Jiang, Q.Y. (2014a), "Power transmission and transformation project establishing and decision-making based on ASU-MOPSO algorithm", *Applied Mechanics and Materials*, Vol. 521, pp. 521-529.

Wei, Y.D., Lai, X.B., Chen, D.Z. and Shen, G.Q. (2006), "Optimal parameters design of two-stage vibration isolation system", *Journal of Zhejiang University (Engineering Science)*, Vol. 40 No. 5, pp. 893-898.

Yan, J.K. (1985), *Mechanical Vibration Isolation Technology*, Shanghai Science and Technology Literature Press, Shanghai, pp. 328-359.

Further reading

Sun, Y., Djouani, K., van Wyk, B.J., Wang, Z. and Siarry, P. (2014), "Hypothesis testing-based adaptive PSO", *Journal of Engineering, Design and Technology*, Vol. 12 No. 1, pp. 89-101.

Appendix

Equation (6) can be derived in detail as follows:

$$\begin{aligned}\Omega_{21} &= \frac{1}{k_1 + ic_1\omega} + \frac{1}{k_2 + ic_2\omega} - \frac{m_1\omega^2}{(k_1 + jc_1\omega)(k_2 + jc_2\omega)} \\ &= \frac{n_1k_2 + k_2 + jn_2c_2\omega + jc_2\omega - um_2\omega^2}{n_1k_2^2 + jn_1k_2c_2\omega + jk_2n_2c_2\omega - n_2c_2^2\omega^2}\end{aligned} \tag{A1}$$

The numerator and denominator of equation (A1) are, respectively, divided by m_2:

$$= \frac{n_1\omega_{n2}^2 + \omega_{n2}^2 + jn_2\omega \times (2\xi_2\omega_{n2}) + j \times 2\xi_2\omega_{n2}\omega - u\omega^2}{n_1k_2\omega_{n2}^2 + jn_1k_2\omega \times 2\xi_2\omega_{n2} + jk_1n_2\omega \times 2\xi_2\omega_{n2} - n_2\omega^2 \times (2\xi_2\omega_{n2})c_2} \tag{A2}$$

The numerator and denominator of equation (A2) are, respectively, divided by ω_{n2}^2:

$$\frac{n_1 + 1 - u\theta^2 + jn_2 \times 2\xi_2\theta + j \times 2\xi_2\theta}{n_1k_2 - n_2 \times 2\xi_2c_2\theta\omega + jn_1k_2 \times 2\xi_2\theta + jk_2n_2 \times 2\xi_2\theta} \tag{A3}$$

Denote:

$$\begin{aligned}A_1 &= n_1 + 1 - u\theta^2; \\ A_2 &= n_2 \times 2\xi_2\theta + 2\xi_2\theta; \\ A_3 &= n_1k_2 - n_2 \times 2\xi_2c_2\theta\omega; \\ A_4 &= n_1k_2 \times 2\xi_2\theta + k_2n_2 \times 2\xi_2\theta.\end{aligned}$$

$$\begin{aligned}\Omega_{22} &= -\frac{m_2\omega^2}{k_1 + ic_1\omega} + \left(1 - \frac{m_1\omega^2}{k_1 + jc_1\omega}\right)\left(1 - \frac{m_2\omega^2}{k_2 + jc_2\omega}\right) \\ &= \frac{\begin{array}{r}-m_2k_2\omega^2 - jm_2c_2\omega^3 + n_1k_2^2 + jn_1k_2c_2\omega + jn_2k_2c_2\omega - n_2c_2^2\omega^2 \\ - n_1k_2m_2\omega^2 - jn_2c_2m_2\omega^3 - um_2k_2\omega^2 - jum_2c_2\omega^3 + um_2^2\omega^4\end{array}}{n_1k_2^2 + jn_1k_2c_2\omega + jn_2c_2k_2\omega - n_2c_2^2\omega^2}\end{aligned} \tag{A4}$$

The numerator and denominator of equation (A4) are, respectively, divided by m_2^2:

$$\frac{\begin{array}{c}-\omega^2{\omega_{n2}}^2 - j\omega^3 \times 2\xi_2\omega_{n2} + n_1{\omega_{n2}}^4 + j\omega{\omega_{n2}}^2 \times 2\xi_2\omega_{n2} + jn_2\omega{\omega_{n2}}^2 \\ \times 2\xi_2\omega_{n2} - n_2\omega^2 \times (2\xi_2\omega_{n2}) - u\omega^2{\omega_{n2}}^2 - ju\omega^3 \times 2\xi_2\omega_{n2} + u\omega^4\end{array}}{n_1{\omega_{n2}}^4 + jn_1\omega{\omega_{n2}}^2 \times (2\xi_2\omega_{n2}) + jn_2\omega \times 2\xi_2{\omega_n}^3 - n_2\omega^2 \times (2\xi_2\omega_{n2})^2} \tag{A5}$$

The numerator and denominator of equation (A5) are, respectively, divided by ${\omega_{n2}}^4$:

$$\frac{\begin{array}{c}-\theta^2 + n_1 - n_1\theta^2 - u\theta^2 + u\theta^4 - n_2 \times (2\xi_2)^2\theta^2 - j2\xi_2\theta^3 + jn_1 \\ \times 2\xi_2\theta + jn_2 \times 2\xi_2\theta - jn_2 \times 2\xi_2\theta^3 - ju \times 2\xi_2\theta^3\end{array}}{n_1 - n_2 \times (2\xi_2)^2\theta^2 + jn_1 \times 2\xi_2\theta + jn_2 \times 2\xi_2\theta} \tag{A6}$$

Denote:

$$\begin{aligned}B_1 &= -\theta^2 + n_1 - n_1\theta^2 - u\theta^2 + u\theta^4 - n_2 \times (2\xi_2)^2\theta^2; \\ B_2 &= -2\xi_2\theta^3 + n_1 \times 2\xi_2\theta + n_2 \times 2\xi_2\theta - n_2 \times 2\xi_2\theta^3 - u \times 2\xi_2\theta^3; \\ B_3 &= n_1 - n_1 \times (2\xi_2)^2\theta^2; \\ B_4 &= n_1 \times 2\xi_2\theta + n_2 \times 2\xi_2\theta.\end{aligned}$$

In summary:

$$\begin{array}{c}\Omega_{21}Z_m + \Omega_{22} = \dfrac{A_1 + jA_2}{A_3 + jA_4}Z_m + \dfrac{B_1 + jB_2}{B_3 + jB_4} = \\ \dfrac{A_1B_3Z_m - Z_mA_2B_4 + A_3B_1 - A_4B_2 + j(A_1B_4Z_m + A_2B_3Z_m + A_4B_1 + A_3B_2)}{A_3B_3 - A_4B_4 + j(A_3B_4 + B_3A_4)}\end{array} \tag{A7}$$

Denote:

$$\begin{aligned}C_1 &= A_1B_3Z_m - Z_mA_2B_4 + A_3B_1 - A_4B_2; \\ C_2 &= A_1B_4Z_m + A_2B_3Z_m + A_4B_1 + A_3B_2; \\ C_3 &= A_3B_3 - A_4B_4; \\ C_4 &= A_3B_4 + B_3A_4.\end{aligned}$$

Then the equation (6) is obtained.

Corresponding author
Wei Huang can be contacted at: huangweiac@126.com